Chapter 6

Charge Transfer in Wet Polymers

ADVANCED MATERIALS 19, 3257 (2007)

In the previous chapters we have investigated the interaction between ions in solution, followed by the interaction between molecules (e.g. amino acids) and the solvent, as well as the complex formation between ions and molecules in solution. In this chapter, the focus will be on charge transfer in a wet polymers at atmospheric pressure using the LIQUIDROM setup. The charge transfer between tetrafluoro-tetracyanoquinodimethane (F4TCNQ), and poly(3-hexylthiophene) (P3HT) will be probed using NEXAFS at atmospheric helium pressure and room temperature. The spectra will be explained by the mean of DFT technique using StoBe DeMon program [12]. These results on the electronic structure are correlated with conductivity measurements carried out at the University of Potsdam.

6.1 Introduction

Doped conjugated polymers can exhibit exceptionally high conductivity > 103 S/cm [154–156]. Here, doping refers to the formation of charge transfer complexes (CTCs) or salts by combining appropriate pairs of donors and acceptors. Similar phenomena can be found in crystalline CTCs comprising small molecules [157–160]. For several decades, the nature of charge transfer and the dimensionality of charge transport in conducting polymers and small molecular crystals have been in the focus of research. For instance, the degree of charge transfer (CT) influences conductivity and determines whether metallic or insulating character prevails [161, 162], and the strength of inter-chain interactions leads to primarily 1D or 3D electronic properties [163, 164]. In addition, disorder - on a molecular and also mesoscopic scale - has a tremendous impact on these

properties [165]. In fact, only recently true metallic behavior of a doped conjugated polymer was demonstrated by a significantly improved structural quality of thin films [166]. Apart from the interest in fundamental phenomena occurring in such systems, recent progress in the field of organic electronics has intensified the efforts to improve the understanding of conducting polymers, as they are a key element for the successful realization of printed all-organic (opto-) electronic devices [167,168]. At present, various mixtures of poly(ethylenedioxythiophene)/ poly(styrenesulfonate) dominate in applications [168–170]; however, it should be interesting to develop alternative conducting polymers, which are not based on an aqueous dispersion and thus allow for new processing options and functionality [171, 172]. A most widely studied class of semiconducting polymers that can be rendered conducting upon doping (so far with inorganic acceptors) is based on polythiophene [156, 173], which has donor character; tetrafluoro-tetracyanoquinodimethane (F4TCNQ, in Fig.6.1.a) is one of the strongest known molecular electron acceptors, and has been used for doping of molecular organic semiconductors [161, 162, 174–176]. Consequently, the prototypical soluble polythiophene variant poly(3-hexylthiophene) (P3HT, in Fig.6.1.b) and F4TCNQ form CTCs, with high conductivity in thin films. Due to the flexibility of the polymer chains and the manifold of possible inter-chain interactions, a large number of different local conformations in P3HT/F4TCNQ CTCs can be expected, leading to large variations of the electronic structure and transport properties within a macroscopic sample.

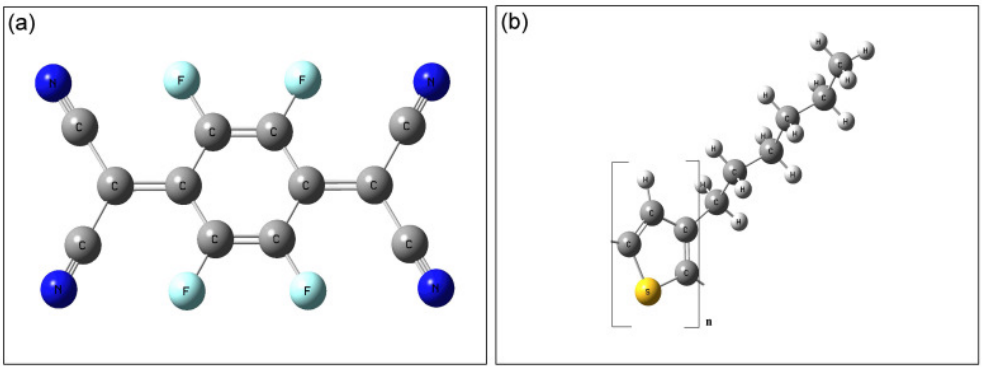

Figure 6.1: Chemical structure for F4TCNQ (a), and P3HT (b).

6.2 Results and Discussion

6.2.1 Electrical Conductivity

The electrical conductivity of P3HT/F4TCNQ thin films was investigated at Universität Potsdam, Institut für Physik, by Mr. P. Pingel, and Prof. D. Neher in thin film transistor geometry with top source and drain contacts (Au) and a bottom gate electrode (n-doped Si). P3HT/F4TCNQ layers were formed by spin-coating from a 1 mg/ml chloroform solution onto silicon substrates, which are covered with an insulating SiO_2 layer (300 nm). Prior to processing, the SiO_2 surface was thoroughly cleaned with several common solvents and an oxygen plasma treatment, followed by silanization using hexamethyldisilazane (HMDS) for 26 hours at 60°C. Device characteristics were recorded using a Keithley 2400 source meter. Sample preparation and measurements were performed in N_2 atmosphere. While pure P3HT layers exhibited clear transistor behavior, the electrical characteristics of the P3HT/F4TCNQ layers were purely ohmic. In this case, the conductivity was calculated from the linear output characteristics (drain current versus drain-source voltage) of the device, and the film thickness (typically 10 nm, measured with a DEKTAK3 surface profiler). Schematic presentation for the conductivity measurement device presented in Fig.6.2.

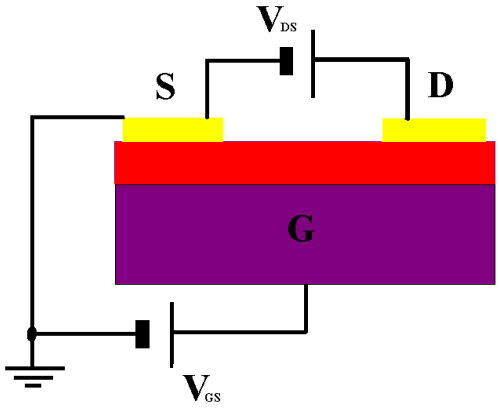

Figure 6.2: Schematic presentation for the conductivity measurement device.

Thin films of F4TCNQ doped P3HT prepared from solution exhibited a dc conductivity of typically 1 S/cm, which corresponds to an increase by 5 orders of magnitude compared to pristine P3HT. This is lower than the reported conductivity of 30 S/cm for ClO_4^- doped P3HT [173]. It was proposed

that in such samples conduction happens primarily along single polymer chains due to weak inter-chain coupling. Interestingly, the conductivity of the P3HT/F4TCNQ films was five orders of magnitude higher than that of dimethylquarterthiophene/F4TCNQ crystals [161], where inter-molecular interactions are strong [177]. In the following the localized character of the CT between P3HT and F4TCNQ is related with the observed conductivity, and it explains the nature of the charge transfer states.

6.2.2 NEXAFS and Theoretical Modeling

F4TCNQ (Aldrich) and P3HT (Aldrich) were dissolved in chloroform (1 mg/ml). In order to form CTCs, both solutions were mixed to have a ratio between F4TCNQ and P3HT-monomers of 1/5. Immediately upon mixing, the color of the solution changed to black, while the pristine solutions were yellow/orange. For NEXAFS measurements, thin films of F4TCNQ and P3HT/F4TCNQ were spin-coated in ambient air onto solvent-cleaned coupons of indium-tin-oxide covered glass. The samples were transferred into the experimental chamber directly after preparation. The resolution of the beamline monochromator was set to 0.1 eV at 400 eV. The spectral fingerprint of residual Nitrogen gas in the chamber was used to calibrate the photon energy, as shown in Fig.6.3. X-ray absorption spectra were recorded in fluorescence yield (FY) mode using a Gallium Arsenide photodiode of $5\times5\ mm^2$ active area.

Details information about DFT simulation for NEXAFS spectra using StoBe is given in section 2.2.2. Specifically for this study, where the nitrogen K-edge is probed, a broadening of 0.5 eV full width at half maximum (FWHM) below 394.5 eV is used, which increases linearly to 0.8 eV at 405 eV. This energy dependent FWHM reflects the fact that the final state broadening is energy dependent due to the increasing number of decay channels for increasing final state energy. For calculating the NEXAFS spectrum of neutral F4TCNQ the reported crystal structure is used as input for the Z-matrix [178]. DFT was used to model the ground state of the P3HT/F4TCNQ charge transfer complex. In order to approximate P3HT, quarterthiophene (4T) was used in the calculations. Geometry optimization was done with the Gaussian03 program package [14], using the B3LYP functional, and a augmented-double Zeta basis set. The optimized geometry was then used as Z-matrix input for StoBe-deMon to calculate the NEXAFS spectrum. It should be noted that DFT may give inaccurate values for the charge transfer [179]. Therefore, to insure

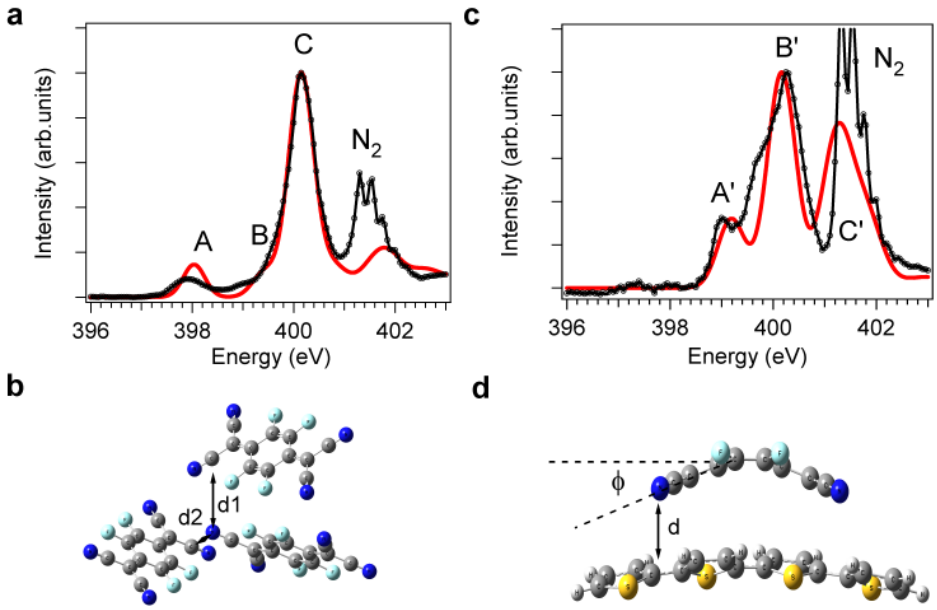

Figure 6.3: Experimental NEXAFS spectra (lines with data points) compared to simulated spectra (solid line) for (a) F4TCNQ, and (c) for P3HT/F4TCNQ. The sharp structures labeled $'N_2'$ are due to residual N_2 gas in the experimental chamber. (b) Model of the arrangement of F4TCNQ molecules in the crystal structure (with distances d1 = 5.1 $\mathring{A}$ and d2 = 4.2 $\mathring{A}$), and (d) the optimized geometry of the model 4T/F4TCNQ CTC obtained by DFT calculations; optimized distance d = 3.53 $\mathring{A}$, and optimized bending angle $\phi = 17.3°$.

that the good agreement between the theoretical spectra and the experimental ones not due to error cancellation in the simulation, the charge transfer varied systematically by changing the distance between F4CTNQ and 4T. Furthermore, using semi-empirical methods (AM1, and PM3) yielded qualitatively similar results.

The NEXAFS spectrum of neutral F4TCNQ exhibits three main spectral features, peaks A, B, and C Fig.6.3.a. Using just a single F4TCNQ molecule as input for theoretical NEXAFS spectral simulation failed. Apparently, F4TCNQ spin-coated from solution forms small crystallites on ITO, as the experimental spectrum could nicely be reproduced theoretically by including the nearest-neighbor inter-molecular interaction present within the F4TCNQ bulk crystal [180]. It turns out that inter-molecular coupling between neighboring

F4TCNQs, in particular mediated by the cyano-groups Fig.6.3.b, is essential for a realistic description of the x-ray absorption process. Analysis of the theoretical results allows to associate peaks A, B, and C to transitions into the lowest unoccupied molecular orbital (LUMO), LUMO+1, and LUMO+2, respectively. The simulated spectrum showed another peak at 401.8 eV, which is most likely superimposed in the experiment by the strong vibrationally resolved absorption of N_2 at the same energy. The fact that including inter-molecular interactions in the theoretical description is essential for reliable modeling provides justification for using the applied methodology.

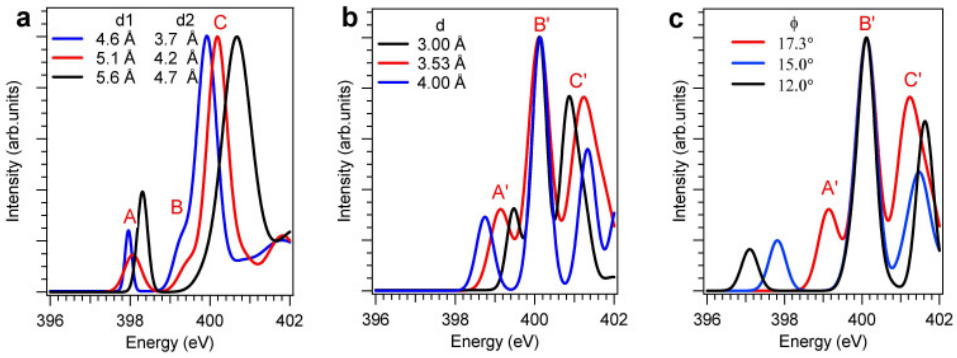

Figure 6.4: Demonstration of the sensitivity of the optimized structures toward changed conformations of F4TCNQ: (a) For neutral F4TCNQ, variation of the inter-molecular distances (in the crystal structure: d1 = 5.1 $\mathring{A}$ and d2 = 4.2 $\mathring{A}$). (b) 4T/F4TCNQ variation of intermolecular distance d (optimized: 3.53 $\mathring{A}$). (c) Variation of ϕ (optimized: 17.3°).

Mixed films of F4TCNQ and P3HT give the NEXAFS spectrum presented in Fig.6.3.c. At first glance, the low energy peak A from Fig.6.3.a, assigned to transitions to the LUMO of neutral F4TCNQ, seems to have disappeared, which might be expected due to electron transfer from P3HT to F4TCNQ, i.e., filling of the neutral F4TCNQ LUMO. However, such a simplistic assignment is misleading, and accurate theoretical modeling is needed to describe the factual interaction in the CTC and the resulting absorption spectrum. Due to computational constraints, the polymer was approximated by quarterthiophene (4T). The optimized structure of the 4T/F4TCNQ model (Fig.6.3.d) reveals that F4TCNQ is strongly twisted compared to its planar neutral form, and the cyano groups bent down toward 4T (which is also non-planar). The optimized model gives a distance d = 3.5 $\mathring{A}$ (as indicated in Fig.6.3.d), and a bending-angle

ϕ of 17.3°. This model allows reproducing the experimental NEXAFS spectrum very satisfactorily, as can be seen in Fig.6.3.1. In order to manifest the accuracy of the DFT-derived CTC conformation, the NEXAFS spectra for systematically changed bond lengths and bending-angles are simulated in (Fig.6.4). Changing the inter-molecular distances by Δd = 0.1 $\mathring{A}$ in either direction from the optimized value results in spectra that do not reproduce the experimental ones. This is the case for both neutral F4TCNQ (Fig. 2a) and the CTC (Fig.6.4.b). Moreover, changing ϕ by >1° from the optimized one results in poor agreement as well (Fig.6.4.c). Note that ϕ values larger than 18° resulted in non-convergence of the calculation. One can conclude from this test that the optimized geometry, which obtained from DFT, explains well our experimental observation and is representative of the conformation of interacting F4TCNQ and P3HT. A full understanding of the charge transfer mechanism could be obtained by analyzing the shape of 4T/F4TCNQ orbitals, and comparing them to those of the isolated donor and acceptor molecules. It turns out that the highest occupied molecular orbital (HOMO) and the LUMO of the F4TCNQ/4T complex are formed by hybridization of the 4T HOMO and the F4TCNQ LUMO (see Fig.6.5). This is a straightforward consequence of the charge transfer, which depletes the donor HOMO and partially fills the acceptor LUMO. This hybridization of orbitals leads to the opening of an energy gap for the complex, which is thus not metallic. As can further be seen from Fig.6.5, the CTC LUMO+1 is derived from the 4T LUMO, and the CTC LUMO+2 and LUMO+3 are reminiscent of the F4TCNQ LUMO+1 and LUMO+2, respectively. With the knowledge about the unoccupied orbital sequence of the CTC, the absorption features in Fig.6.3.c can be assigned. Peak A' is due to an absorption process into the CTC LUMO, peak B' into the LUMO+2, and peak C' into the LUMO+3. Transitions from the F4TCNQ N1s level into the LUMO+1 of the CTC are not observed, as this orbital is localized on 4T. Importantly, the charge transfer and the associated orbital hybridization have essentially resulted in a shift of the N-edge NEXAFS spectrum toward higher energies, and not simply to the disappearance of the F4TCNQ LUMO, as noted above.

6.3 Conclusion

Summarizing the previous results give the following picture: the charge transfer interaction between F4TCNQ and P3HT is very strong, leading to significant molecular conformation changes, and rather localized on approximately four

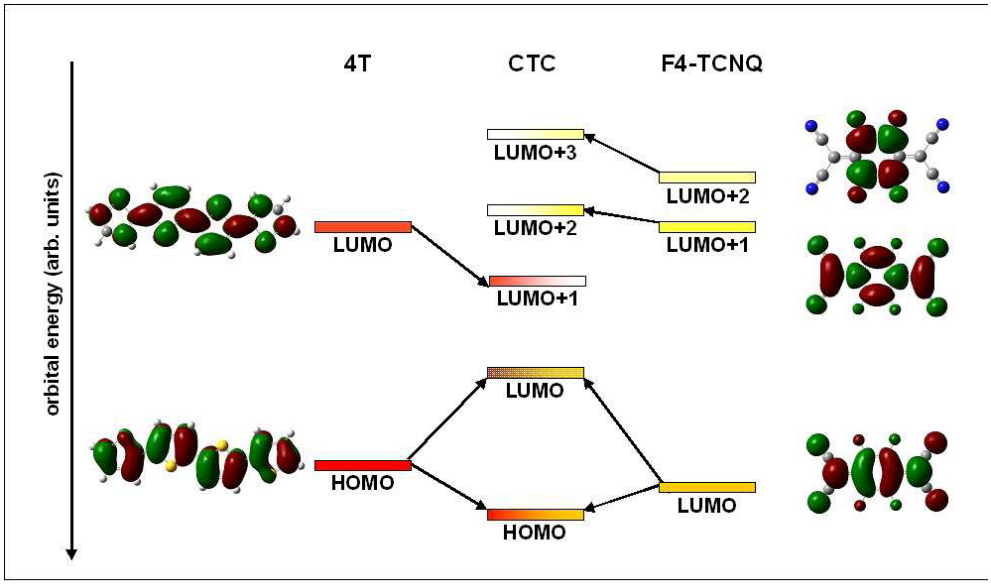

Figure 6.5: Schematic energy level diagram of the 4T/F4TCNQ charge transfer complex (CTC) and its constituent molecules obtained from orbital analysis of theoretical modeling, evidently showing the hybrid character of the CTC HOMO and LUMO

repeat units of a single donor polymer chain. Inter-chain interactions seem not to play a dominant role in this case. The HOMO and LUMO levels of the CTC, which are relevant for charge transport, are formed by hybridization of the donor HOMO and the acceptor LUMO, and due to the finite energy gap the complex is non-metallic. Yet, as the conductivity of thin P3HT/F4TCNQ films was high (1 S/cm), much more free charge carriers can be generated in doped samples compared to the pristine polymer at room temperature. In the future it will be interesting to test if higher conductivity in all-organic molecularly doped conjugated polymers can be achieved by either reducing the strength of donor/acceptor charge transfer, or by increasing inter-chain interactions. Both strategies may result in a less localized character of the charge transfer, which is an important criterion for achieving high conductivity. The availability of more tailor-made highly conducting polymers, which can be directly processed from solution on large areas, would have a tremendous impact on advancing the field of plastic electronics.

Most notably, only one specific CTC conformation has been found to be predominates, where F4TCNQ is strongly bent out of its neutral planar

form due to pronounced electron donation from P3HT chain segments. In contrast, in a related F4TCNQ/oligothiophene charge transfer crystal F4TCNQ remained planar because of dominant inter-molecular interactions in an ordered environment [177]. Furthermore, the energy levels of the CTC are clearly shown to be hybrids of the individual levels of the separate donor and acceptor molecules. This indicates that the CT in P3HT/F4TCNQ is highly localized and does not involve significant inter-chain interactions. Consequently, this system should exhibit 1D transport properties, with possibly reduced carrier mobility due to the localized donor-acceptor interaction [178]. In fact, the strength of interaction, expressed by the significant molecular conformation changes, leads to a self-localization of charges. Decreasing the local character of organic/organic CTCs or increasing inter-molecular interactions may thus be strategies to achieve even higher conductivity.